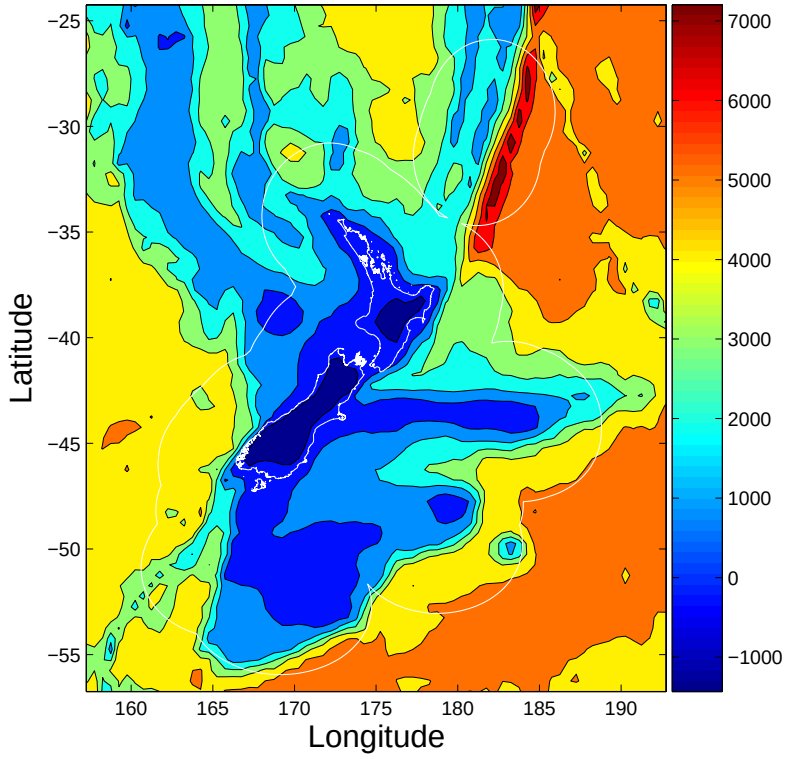

Figure 3.3: Contour plot of the bathymetry (bottom depth in metres) in the New Zealand EEZ region. The NZ coastline and EEZ boundaries are shown in white.

3.11 EEZ boundaries

The New Zealand Exclusive Economic Zone (EEZ) is made up of the sea, seabed and subsoil within 200 nautical miles of the baseline, which in most cases is defined as the low-water mark around the coasts of both mainland New Zealand and its outlying islands. In places this area overlaps with the Australian EEZ. The boundary between the EEZs will be established by the 'Australia-New Zealand Maritime Delimitation Treaty' which was signed in July 2004.

The boundary of the New Zealand EEZ was downloaded from the Land Information New Zealand web site (http://www.hydro.linz.govt.nz/boundaries/downloads/eez-download.asp).

3.12 Calculation of CCD and ELD

Figure 3.4 shows the dependence of the calculated saturation index Ω for both calcite and aragonite on bathymetric pressure for a typical station in the data set. For both $CaCO_3$ polymorphs, there is a steady decrease in the value of Ω with increasing pressure, with aragonite showing a smaller pressure for saturation (Ω = 1) than calcite, as expected. For calcite, the dependence of Ω on pressure is seen to be almost exactly linear in the pressure region spanning $0.6 < \Omega < 1.4$ (in this case $r^2 = 0.995$), allowing a simple estimate of the CCD (Ω = 1) using linear regression. This feature was universally observed for the WOCE P14S and P15S data, at least for latitudes greater than 20°S. The reason for this linear trend is not known at present.

For aragonite, the plot of Ω *vs* pressure is not linear near Ω = 1, precluding the use of linear regression for estimating the CCD for this polymorph. Thus in this case linear interpolation using the two nearest point bracketing Ω = 1 must be used. However, CCD values for aragonite were not included in this report.

The standard error in the value of the CCD for calcite was estimated from the standard errors in the slope and intercept of the regression line. For the 88 stations for which a CCD was calculated, the average standard error was ± 94 dbar. Some stations did not have data for depths greater than the CCD so a value could not be evaluated (10 stations).

It should be noted that the units of CCD as calculated from these results are in dbar, which is numerically close to the actual depth in metres. The relationship between pressure in dbar and depth in metres varies slightly with latitude. However, this conversion was not carried out for this report because the uncertainties in the estimate of CCD as noted above are too large to make the difference between pressure and depth of any consequence.

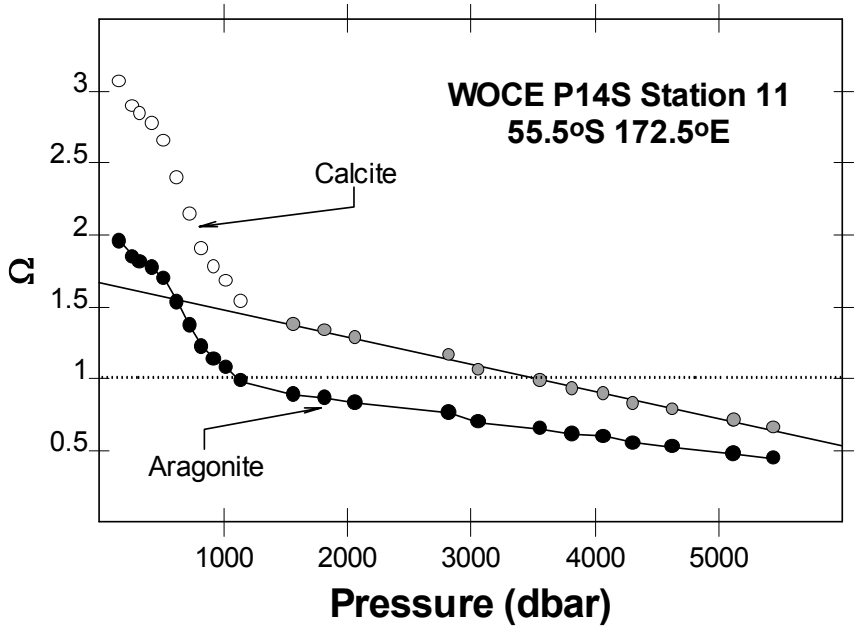

Figure 3.4: Dependence of saturation index Ω for calcite and aragonite for station 11, WOCE P14S.

Figure 3.5 shows the calculated CCD for all stations in P14S and P15S as a function of latitude. These results demonstrate very little difference between the CCD for the two cruises having common latitudes, indicating that at least at these latitudes, the CCD is a longitudinally homogeneous feature of the South Pacific.

The results show a peak at ~ 57°S, which corresponds to the Antarctic Convergence, decreasing sharply at higher latitudes and more steadily towards lower latitudes (i.e. towards the equator). These trends are as expected. The primary process controlling CCD is the strength of the biological pump system, which drives the products of phytoplankton respiration along the oceanic conveyor belt (refer Introduction). Thus a steady decrease in CCD northwards seen from ~ 57°S is consistent with increasing water mass age going from South to North in the Pacific. The substantially lower CCD south of ~ 57°S must be a result of more intense water column overturn south of the Antarctic Convergence which should lead to a shallowing of the CCD.

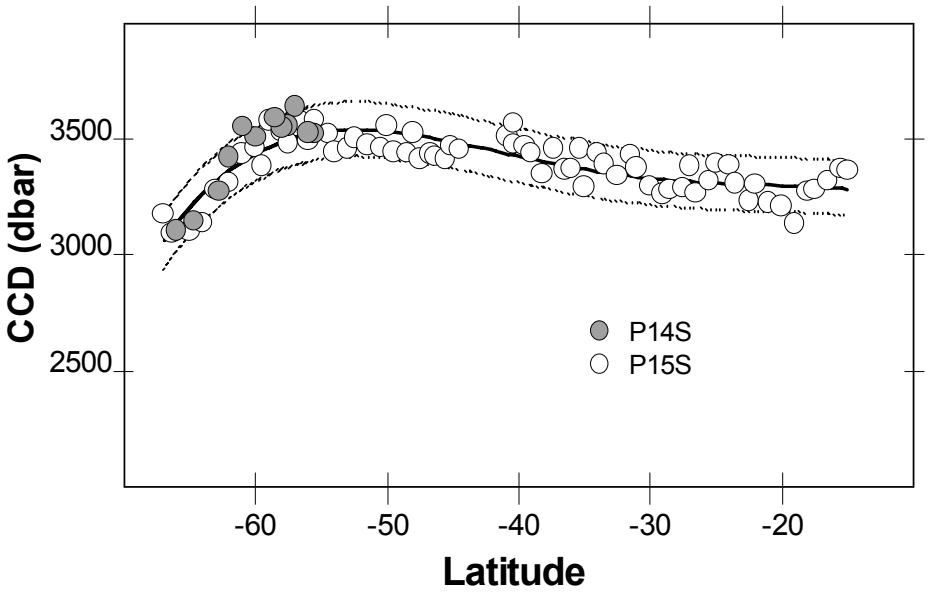

Figure 3.5: Calculated CCD for calcite for P14S and P15S as a function of latitude. The solid line represents the 4th order polynomial used to parameterize CCD in terms of latitude. The dotted lines represent error limits estimated at ± 59 dbar.

The CCD results in Figure 3.5 were fitted to a 4th order polynomial in latitude in order to parameterize CCD.

$$\text{CCD} = a_0 + a_1 L + a_2 L^2 + a_3 L^3 + a_4 L^4 \qquad [3.7]$$

where $a_0 = 2867 \pm 449$, $a_1 = -64 \pm 52$, $a_2 = -3.50 \pm 2.13$, $a_3 = -0.082 \pm 0.036$ and $a_4 = -0.00065 \pm 0.00022$ (error values are the standard errors derived from the least-squares fitting). This equation explained 71% of the variation in CCD.

The mean absolute difference between actual and fitted CCD values for the data set was 59 dbar and this is represented by the dotted lines in Figure 3.5. It can be seen that the envelope defined by these error limits encompasses most of the actual CCD values. This is the likely error in the CCD values reported here.

For the ELD, i.e. pressure at which $\Omega = 0.8$, a similar approach was taken. Compared to the CCD, fewer stations were deep enough to have Ω values smaller than 0.8, allowing evaluation of ELD. Figure 3.6 shows how the calculated ELD values depend on latitude for both WOCE cruises. The general features of these results are very

similar to those observed for the CCD, except that the estimated lysocline depth ELD is approximately 900 dbar deeper than the calcite compensation depth CCD.

The coefficients for the 4th order fitting of ELD to latitude were $a_0 = 2136 \pm 628$, $a_1 = -300 \pm 73$, $a_2 = -13.40 \pm 2.97$, $a_3 = -0.2511 \pm 0.0504$ and $a_4 = -0.001690 \pm 0.00030$ and this polynomial explained 79% of the variance in ELD.

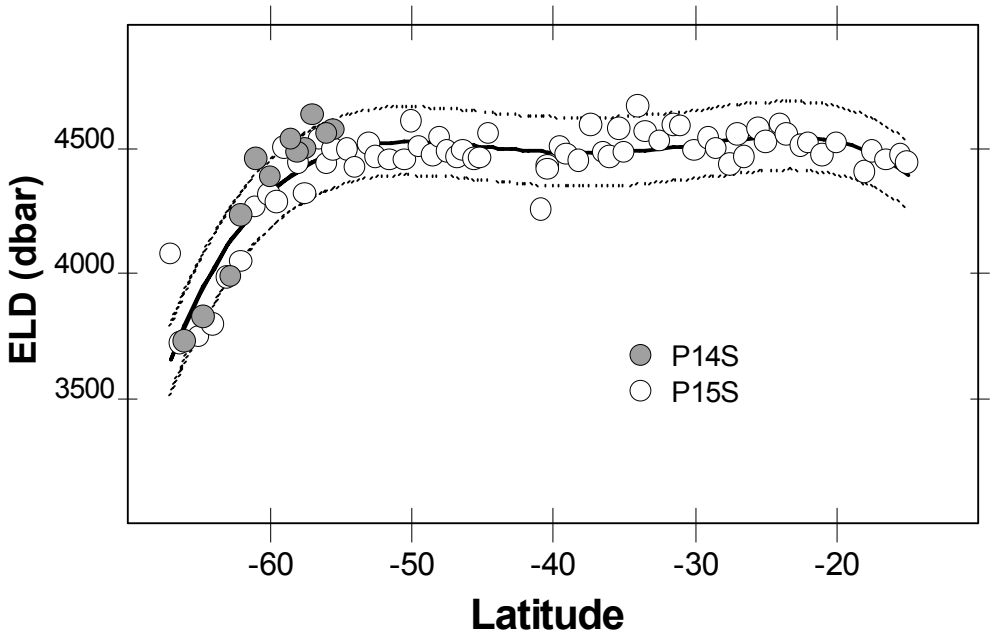

Figure 3.6: Calculated ELD for calcite for P14S and P15S as a function of latitude. The solid line represents the 4th order polynomial used to parameterize CCD in terms of latitude. The dotted lines represent error limits estimated at ± 68 dbar.

Figure 3.7 shows a plot of the difference between the calculated ELD and CCD as a function of latitude for P14S and P15S. This reveals that the difference increases towards the equator from about 800 dbar at the southernmost latitudes to about 1200 dbar at 20°S. This trend is probably also related to the biological pump system which seems to affect the CCD more than the ELD. Figure 3.5 shows that CCD decreases towards the equator whereas the ELD remains approximately constant (Figure 3.6).

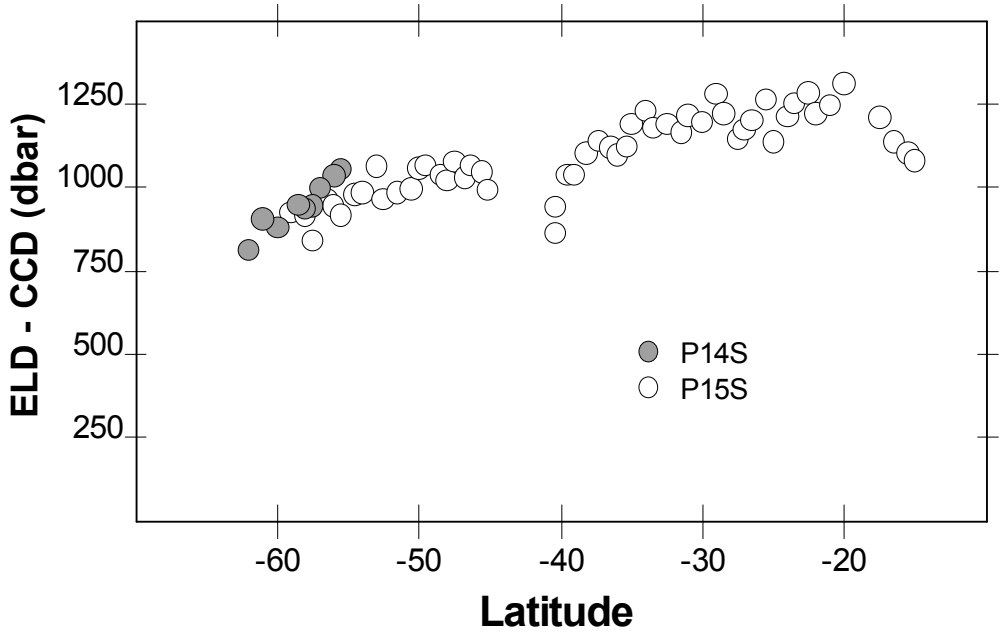

Figure 3.7: Difference between calculated ELD and CCD for calcite for P14S and P15S as a function of latitude.

3.13 Mapping of the CCD and ELD

In the absence of any additional data on the CO_2 system in the grid area, the only reasonable assumption that can be made is that the CCD is uniformly distributed with respect to longitude in the range 157°E to 167°W with a latitudinal dependence given by the results in Figure 3.5 for CCD and Figure 3.6 for ELD. These calculated values were then clipped against the bathymetry by taking whichever of the CCD and bottom depth was shallower for each grid square.

The results for CCD are shown as a contour plot in Figure 3.8. The detailed results show that over most of the EEZ region the bottom depth is shallower than the calculated CCD. Indeed, it is only in the outermost extremes to the east and west of the EEZ where the seafloor is deeper than the CCD.

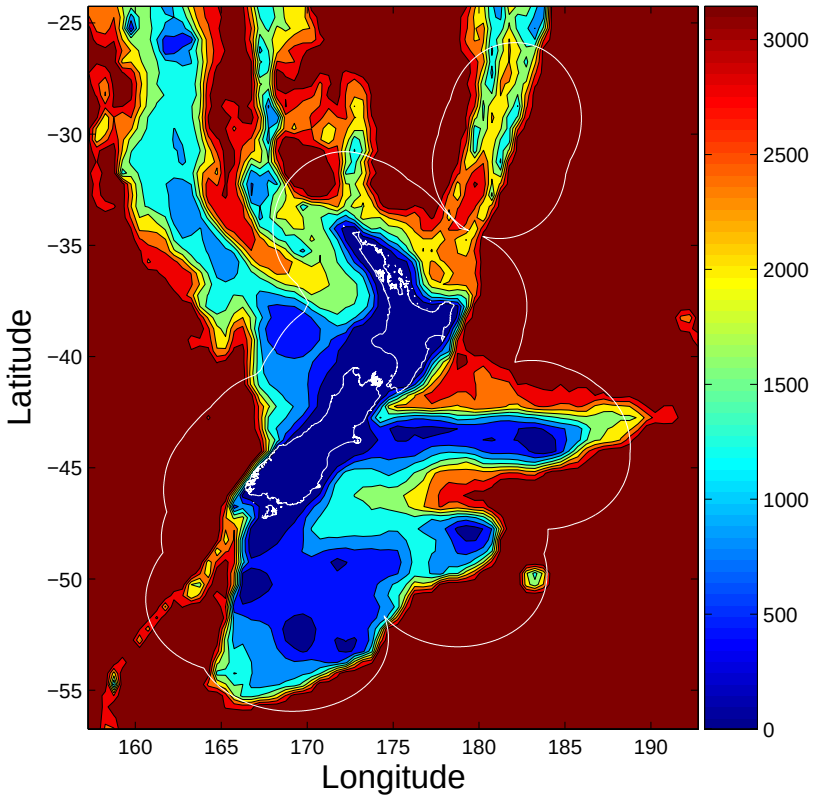

Figure 3.8: **Contour plot of either the CCD or the bottom depth, whichever is shallower, for the NZ oceanic region. The NZ coastline and EEZ boundaries are shown in white.**

The Estimated Lysocline Depth (ELD) was contoured in a similar way, with the results shown in Figure 3.9. Since the ELD is approximately 900 dbar deeper than the CCD, even more of the sea floor is shallower than this horizon than was the case with the CCD, with the result that Figure 3.9 is very similar to the bathymetric map (Figure 3.3).

Continue to next file: MCU6b